Deep-Etch Visualization of 27S Clathrin: A Tetrahedral Tetramer

J. E. Heuser,* J. H. Keen,‡ L. M. Amende,§ R. E. Lippoldt,§ and K. Prasad§

*Department of Cell Biology and Physiology, Washington University School of Medicine, St. Louis, Missouri 63110; ‡Fels Research Institute and the Department of Biochemistry, Temple University School of Medicine, Philadelphia, Pennsylvania 19140; and §Clinical Endocrinology Branch, National Institute of Diabetes, Digestive, and Kidney Diseases, National Institutes of Health, Bethesda, Maryland 20892

Abstract. It has recently been reported that 8S clathrin trimers or "triskelions" form larger 27S oligomers upon dialysis into low ionic strength buffers (Prasad, K., R. E. Lippoldt, H. Edelhoch, and M. S. Lewis, 1986, *Biochemistry*, 25:5214–5219). Here, deep-etch electron microscopy of the 27S species reveals that they are closed tetrahedra composed of four clathrin triskelions. This was determined by two approaches. First, standard quick-freezing and freeze-etching of unfixed 27S species suspended in 2 mM 2-(*N*-morpholino)ethane sulfonic acid (MES) buffer, pH 5.9, yielded unambiguous images of tetrahedra that measured 33 nm on each edge. Second, the technique of freeze-drying molecules on mica (Heuser, J. E., 1983, *J. Mol. Biol.*, 169:155–195) was modified to overcome the low affinity of mica in 2 mM MES, by pretreating the mica with polylysine. Thereafter, 27S species adsorbed avidly to it and collapsed into characteristic configurations containing four globular domains, each linked to the others by three ~33-nm struts. The globular domains look like vertices of deep-etched clathrin triskelions and the links, numbering 12 in all, look like four sets of triskelion legs. New light scattering and equilibrium centrifugation data confirm that 27S polymer is four times as massive as one clathrin triskelion. We conclude that in conditions that do not favor the formation of standard clathrin cages, low affinity interactions lead to closed, symmetrical assemblies of four triskelions, each of which assumes a unique puckered, straight-legged configuration to create the edges of a tetrahedron. Tetrahedra are similar in construction to the cubic octomers of clathrin recently found in ammonium sulfate solutions (Sorger, P. K., R. A. Crowther, J. T. Finch, and B. M. F. Pearse, 1986, *J. Cell Biol.*, 103:1213–1219) but are still smaller, involving only half as many clathrin triskelions.

When clathrin-coated vesicles are exposed to 0.5 M Tris pH 7 (13) or 2 M urea (2, 31), their polygonal cages depolymerize into 8S components. These molecules have been named "triskelions" due to their three-legged pinwheel shape (27). Triskelions dissociate further in SDS into three 180-kD and three ~30-kD polypeptides (14, 17, 18, 22, 24, 27), suggesting that each of their three "legs" is composed of one heavy and one light chain. Upon dialysis back into physiological ionic strength buffers, especially when the buffers are slightly acidic and when divalent cations are present, triskelions reassemble spontaneously into empty "cages" that approximate the size and shape of the original vesicle coats (1, 4, 13, 28, 31, 32). Such empty cages sediment at ~150–300S (17–21, 25, 27, 28). If the dialysis conditions are altered, two smaller clathrin polymers will form, one sedimenting at ~42S and one at ~27S. The 42S form occurs only when the dialysis solution also contains >10% saturated ammonium sulfate. Structural studies have shown that this species is a cube composed of eight triskelia (26). In contrast, the 27S polymer apparently only forms when the dialysis solution is very low ionic strength (2 mM in the first report [23]). Equilibrium sedimentation analysis has suggested that the 27S species is a hexamer (23), but structural analyses have not been done.

Here we take advantage of the fact that 27S polymers of clathrin are stable at such low ionic strength that we can deep-etch and platinum-replicate them in suspension. Heretofore, electron microscopic visualization of such small entities by deep-etching has been thwarted by a residuum of salt that forms during etching (the salt forming small granules that obscure small macromolecules, cf. references 8 and 9), but freeze-etching of 2 mM solutions proves to leave very little salt scum. By combining this approach with our more standard technique of attaching molecules to mica and freeze-drying them (9), we have demonstrated that the 27S polymer of clathrin is a tetrahedron composed of four clathrin triskelions, each of which assumes a unique puckered, straight-legged conformation. New equilibrium centrifugation and light scattering data are also presented to support the conclusion that the 27S species is a tetramer, and to correct the earlier claim that it was a hexamer. These results were presented in abstract form earlier (11).

Materials and Methods

Preparation of 8S Clathrin Triskelions

Coated vesicles were purified from calf brains by homogenization and centrifugation as previously described (13). Clathrin was released from coated vesicles with 0.5 M Tris pH 7.0 and separated from assembly polypeptides by chromatography on Sepharose Cl-4B, also as previously described (13).

Polymerization of 27S Clathrin

The 27S polymer was prepared from column-purified clathrin at ~0.1–0.4 mg/ml, by reducing the Tris concentration from 0.5 M, first by overnight dialysis against 10 mM Tris, pH 8.5, and then by overnight dialysis against 2 mM Na-2-(*N*-morpholino)ethane sulfonic acid (MES) buffer, pH 5.9, with repeated changes of the dialysate. For sedimentation equilibrium studies, the solution was sedimented at 30,000 rpm for 30 min in a Ti 70.1 rotor (Beckman Instruments, Inc., Palo Alto, CA) to remove a small percentage (5–10%) of aggregates that sometimes form after dialysis.

Polymerization of 42S Clathrin

The 42S polymer was prepared from column-purified clathrin at ~1 mg/ml, by the procedure introduced in reference 26. This involves overnight 4°C dialysis against 40 mM Tris-HCl pH 7.0, 1 mM EDTA, 0.01% 2-mercaptoethanol, 0.2 mM phenylmethylsulfonyl fluoride (PMSF), followed by a second overnight 4°C dialysis against 0.1 M Na-MES buffer pH 6.0, 1 mM EDTA, 0.2 mM PMSF, and 12% saturated ammonium sulfate. Thereafter, the 42S species appeared to be stable indefinitely.

Electron Microscopy

Electron microscopy of 27S clathrin in suspension was accomplished by placing 10-μl aliquots of 0.4 mg/ml clathrin in 2 mM Na-MES on 4 × 4-mm slabs of fixed rabbit lung (for support) and quick-freezing them by pressure against the liquid helium–chilled copper block of our "Cryopress" (manufactured by Med-Vac, Inc., St. Louis, MO), as previously described (10). The samples were then fractured, etched, and replicated with platinum by slight modifications of our standard procedures (8–10), as indicated in the figure legends. Alternatively, images of 27S and 42S clathrin adsorbed to mica were obtained by prefixing them with glutaraldehyde (40 mM for 10 min at 4°C) and then mixing them with mica chips pretreated with 10 mg/ml low molecular weight polylysine. The rationale for this adaptation of our standard mica-chip procedure is explained in the Results. Thereafter, the slurry of mica chips was quick-frozen, fractured, freeze-dried, and replicated with platinum as described earlier (9, 15). Images were recorded in a transmission electron microscope at 70,000 initial magnification as ±10° stereo pairs and measured by mapping them onto a digitizing tablet while viewing them in three dimensions, as also described earlier (10).

Light Scattering

Light scattering was measured at a wavelength of 430 nm, a temperature of 20°C, and a scattering angle of 90° by using a square cuvette in a fluorometer (model MPF-3; Perkin Elmer Corp., Norwalk, CT). The actual value we measured was Rayleighs ratio (Ir^2/I_0). The relation between this value, the turbidity (τ), and the molecular weight of the sample is given by the following equation (cf. reference 3):

$$\tau = (8\pi/3)\,(Ir^2/I_0) = HCMP(O), \quad (1)$$

where

$$H = (32\pi^3/3N)\,(n_0^2/\lambda^4)\,(dn/dc)^2. \quad (2)$$

Here, C is the concentration (g/ml), N is the Avogadro constant, n_0 is the refractive index of the solvent, dn/dc is the refractive index increment at constant chemical potential, λ is the wavelength, and $P(O)$ is the angular dependence of the scatter known as particle scattering factor.

Analytical Ultracentrifugation

An analytical ultracentrifuge (model E; Beckman Instruments, Inc.) equipped with a photoelectric scanner was used for both velocity and equilibrium studies. Double sector cells, with a 12-mm optical path length, were used for all experiments. Scans were taken at a wavelength of 280 nm.

Velocity experiments were carried out in an AN-F-Ti rotor (Beckman Instruments, Inc.) at a speed of 20,000 rpm and a temperature of 23°C. The radial position of the 50% concentration point of the boundary as a function of time was used to compute the sedimentation coefficient.

Equilibrium experiments were carried out at 5°C using an AN-D rotor at a speed of 3,000 rpm in 2 mM MES, pH 5.9 or 3,600 rpm in 2 mM MES, pH 5.9, 3 M glycerol. Ultracentrifugal equilibrium was considered to have been attained when successive scans became invariant with time. Data were obtained by manually digitizing the scans and converting the *X-Y* coordinates to concentration in the form of optical density at 280 nm as a function of radial position in the cell. These were analyzed by mathematical modeling by nonlinear least-squares curve-fitting using MLAB, an interactive system operating on a DEC-10 computer (see reference 23 for further details). The concentration as a function of radial position at equilibrium was considered to be

$$C_r = \sum_{i=1}^{n} C_{b,i} \exp[AiMi\,(r^2 - r_b^2)] + \varepsilon, \quad (3)$$

where $C_{b,i}$ $(i - 1)$ is the concentration of the ith solute, C_r is the total concentration at any radial position r, M_i is the molecular weight of the ith solute, $A = (1 - \nu\rho)\omega^2/2RT$, ν is the partial specific volume of the protein, ρ is the solution density, ω is the rotor angular velocity, R is the gas constant, T is the absolute temperature, and ε is a small error term to adjust for baseline error. In this equation it is assumed that the partial specific volume ν is the same for all the species present, an approximation that is generally considered to be valid in protein associating systems.

Results

Deep-Etch Electron Microscopy of 27S Clathrin

Shallow etching of a suspension of 27S clathrin polymers in 2 mM MES buffer pH 5.9 yields various views of what appear to be tetrahedra (Figs. 1 and 2). These views include, most notably, equilateral triangles 33 nm on a side (Fig. 2, rows *a–c*). Tetrahedra would of course be composed of four such equilateral triangles. Also common are protruding triangular corners (Fig. 1) and 33-nm straight edges (Fig. 2, rows *f* and *h*); these appear to be partial views of tetrahedra. Finally, a number of forms look like fractured tetrahedra. These include straight edges with knobs at either end, and triangles with knobs at all three corners (Fig. 2, rows *d*, *e*, and *g*). The knobs appear to be the remnants of struts that linked the remaining structures with portions of tetrahedra that were fractured away.

While these images were being produced, a report was published describing another small clathrin oligomer, a 42S species, that apparently forms a cube (26). It thus became of interest to compare the two forms. Figs. 3 and 4 illustrate the deep-etch appearance of 42S clathrin in 12% saturated ammonium sulfate before and after uranyl acetate fixation. The 27S and 42S species prove to have exactly the same edge-lengths (when measured from the center of one vertex to the center of adjacent vertices), namely, 33 nm. They are clearly different, however, in that the 42S species invariably display square faces, whereas the 27S species invariably display triangular faces.

Comparison of these forms with the native clathrin polymer offers additional perspective. Fig. 5 presents the deep-etch appearance of an in situ clathrin polymer, which is seen to be composed of hexagonal and pentagonal facets. Its composite "struts" are substantially thicker than those of the smaller species under study here (10 nm vs. 6 nm after correction for 2 nm of platinum), and its vertices are separated by roughly half the distance found in the smaller species

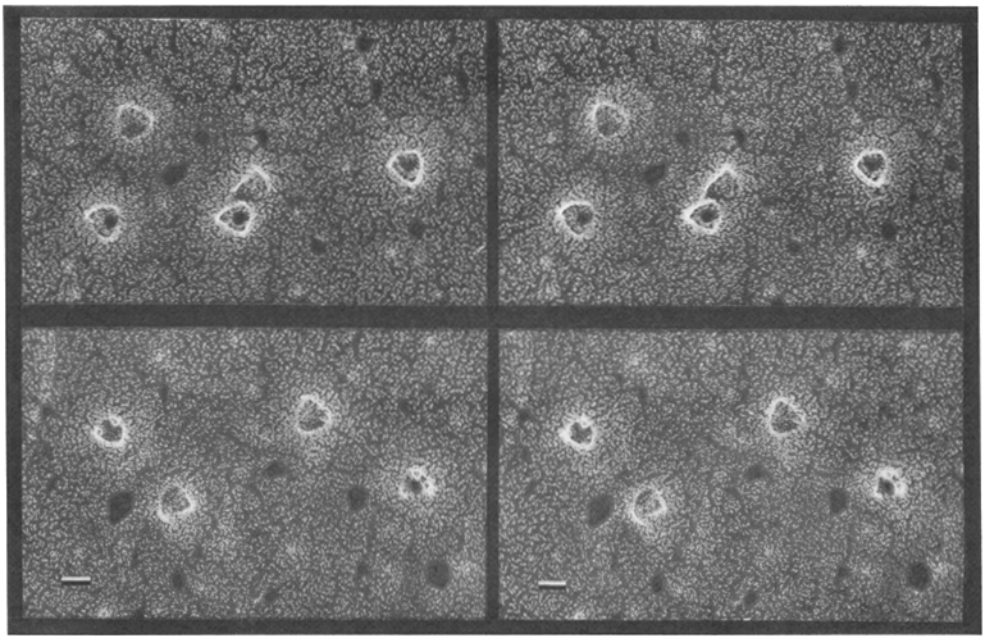

Figure 1. Stereo views of 27S clathrin polymers suspended in 2 mM MES buffer, obtained by etching a quick-frozen solution relatively briefly (1 min rather than the usual 3–4 min at −100°C). This lowered the ice table around the macromolecules by some 50 nm, as compared to the usual exposure of 1/4–1/2 μm in "deep" etching. Bar, 33 nm.

(~16 nm vs. ~33 nm). Isolated 8S clathrin triskelions, by comparison, have still thinner legs (~4 nm) and display characteristic bends in their legs at ~16 nm from their vertices (Figs. 2 and 4, bottom corner panels). Several previous reports have shown that triskelions could fit neatly into the in situ hexagonal lattice (4, 14, 27), but the fit into 27S tetrahedra is not so obvious. Fig. 6 graphically illustrates the problem, by showing individual faces of 27S tetrahedra superimposed upon an in situ hexagonal lattice, both obtained by identically scaled camera lucida tracings of Figs. 2 and 5. Note that vertices in the 27S tetrahedra coincide with nonadjacent vertices in the in situ lattice. The implications of this will be explained below.

Further characterization of the 27S species was performed by adapting them to the mica adsorption/freeze-dry procedure used for the 42S species above. However, there was a problem here. The 27S form of clathrin failed to adhere to mica in very low ionic strengths, but promptly depolymerized when ionic strength was raised during mica exposure. Polylysine pretreatment of the mica increased its affinity for clathrin but caused the 27S polymers to come apart during adsorption, as happens also when normal clathrin baskets adsorb to polylysine mica (10). To avoid this, 27S clathrin was prefixed in 40 mM glutaraldehyde (in 2 mM MES pH 5.9) for 10 min at 4°C and then adsorbed to polylysine-treated mica. This yielded discrete structures on mica (Figs. 7 and 8), which, a first glance, look very little like tetrahedra. Instead, they resemble small jellyfish or medusae (Fig. 8, rows *c* and *d*) or, in terms of their globules-connected-by-strands appearance, like the Bohr models of atomic electron shells (Fig. 8, rows *a* and *b*). Nevertheless, wherever their components are clear and non-overlapping, they can be seen to contain four globules, each connected to all the others by two slightly separated thin strands. When the four globules lie at the four corners of an imaginary square, two pairs of strands crisscross in the center to link them together (thus creating the "atomic" images, Fig. 8, row *b*). In other instances (the "medusae" images; cf. Fig. 8, row *d*), three of the globules lie in a row and the fourth off to one side, its three pairs of strands radiating out in a bell-shape to join the others. These are in fact two of the many possible planar projections of a tetrahedron, assuming each of its vertices forms a globule and each of its edges splits in two during adsorption to mica. Indeed, the globules in question look similar to the vertices of single triskelions adsorbed to mica in low affinity conditions (10, 15), and the strands are the proper width and length to be single triskelion legs (cf. Figs. 2 and 4, *lower panel*). Thus the images of 27S clathrin flattened onto polylysine-mica are additional evidence that the tetrahedron is composed of four clathrin triskelia, one at each vertex, with their legs overlapping in antiparallel arrangement to create each of the tetrahedral edges. Very rarely, variants of this form with only three globules and six interconnecting strands are found in 27S preparations (Fig. 8, row *e*). The predominant tetrameric form is diagrammed in Fig. 9.

The obvious discrepancy between the present interpretation of the 27S species as a tetramer, versus the earlier equilibrium centrifugation data suggesting a hexamer (23), mandated several control experiments to ensure that glutaraldehyde fixation and adsorption to mica did not create tetramers artifactually. To avoid prefixation, we examined several 27S preparations that were exposed to 70 mM KCl for only a few seconds before exposure to mica (the salt being provided to restore mica's affinity). This destabilized the tetrahedra but did not always allow time for complete dissociation (Figs. 10 and 11). Most importantly, the few tetrahedra that remain intact in these preparations (Fig. 10, circled structures) look identical to those observed after fixation and adsorption to polylysine-mica. Furthermore, among the images of partial dissociation are numerous examples of tetrahedra with one or two strands sticking out (Fig. 11, row *a*). These show that each of the two strands that connect adjacent tetrahedral vertices is in fact a single triskelion leg. Also present are many examples of complete dissociation, in which

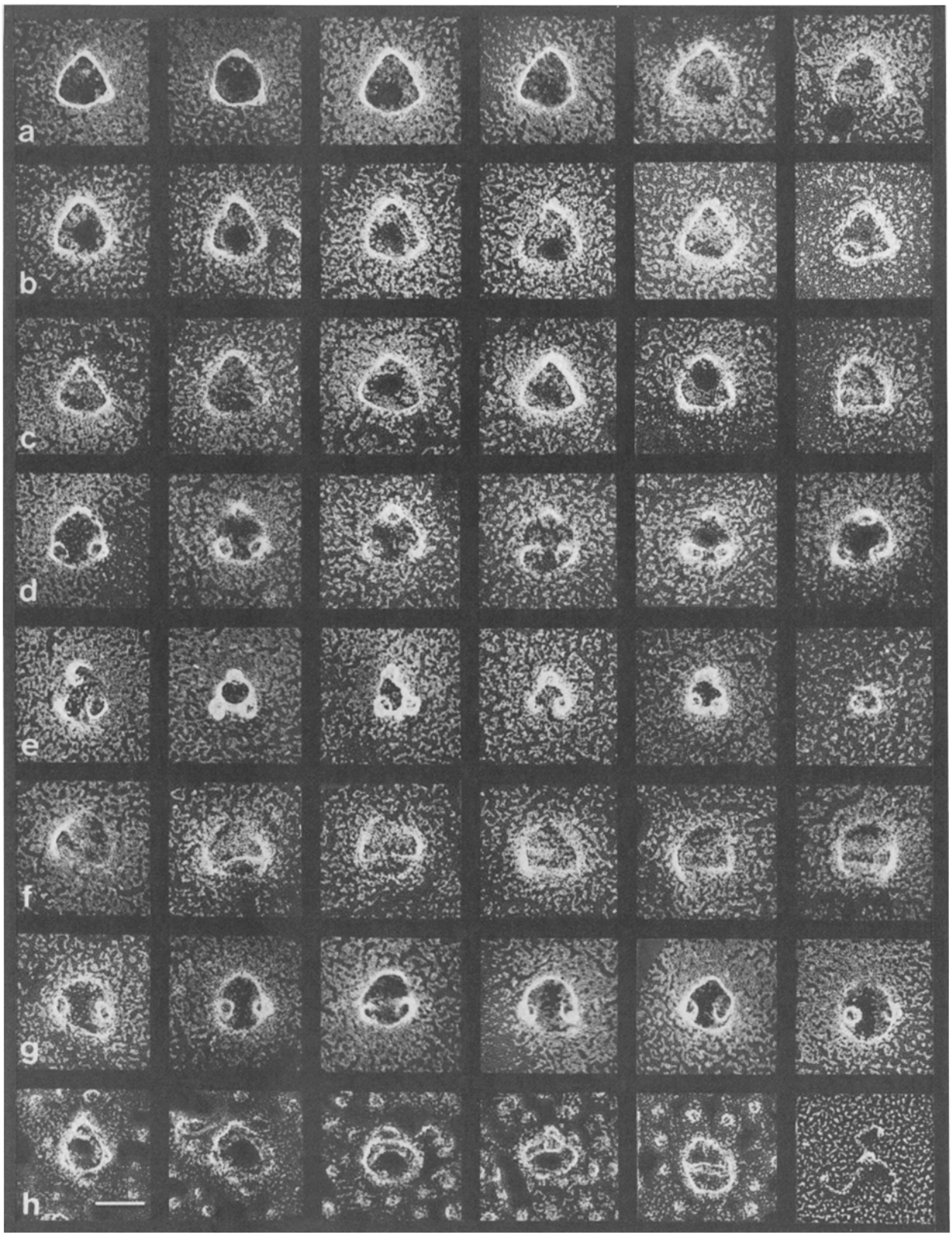

Figure 2. Gallery of different views of 27S clathrin polymers in suspension in 2 mM MES buffer, illustrating their predominantly triangular appearance, consistent with their being one-sided views of 33-nm tetrahedra. Rows *a–c* display intact tetrahedra seen from one triangular face; row *d* displays tetrahedra with their uppermost vertex fractured away; row *e* displays deeper fractures progressively approaching the last vertex embedded in ice; row *f* displays intact tetrahedra seen from one edge while row *g* displays ones with this edge fractured away; and finally, row *h* displays tetrahedra from various vantage points, in this case in 20 mM KCl (the small white dots in the background). In the lower right corner is an 8S clathrin triskelion printed at the same magnification. Bar, 33 nm.

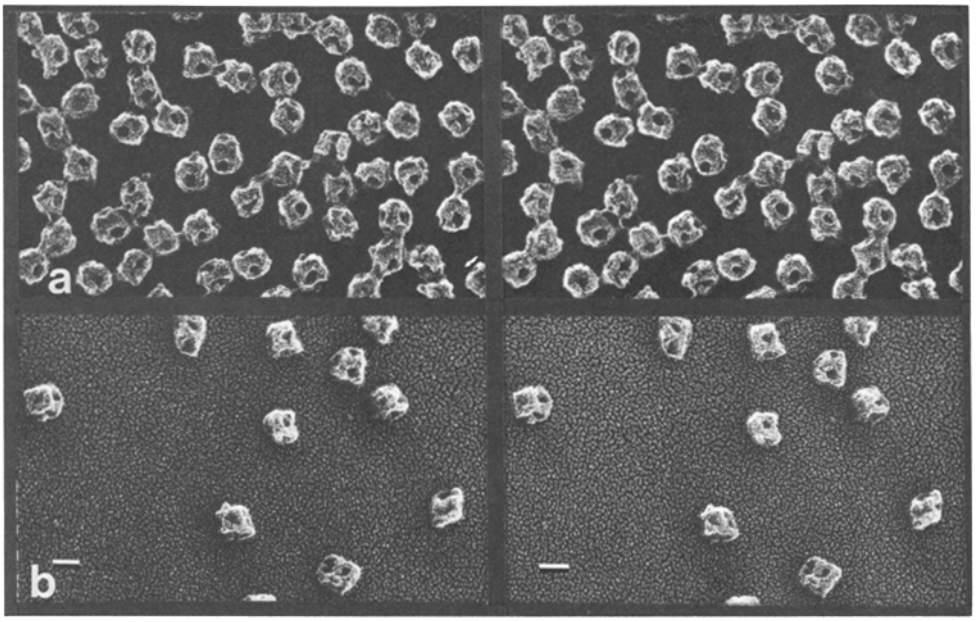

Figure 3. Stereo views of 42S clathrin polymers adsorbed to mica in 12% saturated ammonium sulfate and then either quick-frozen directly (*a*) or washed with 0.5% uranyl acetate in 12% saturated ammonium sulfate and then washed in water (*b*). In *a*, the cubic form of these polymers is readily apparent, in spite of a thick layer of residual ammonium sulfate. In *b*, the salt has been washed away. This has also removed a large proportion of the cubes but has left the remaining ones much cleaner. Bar, 33 nm.

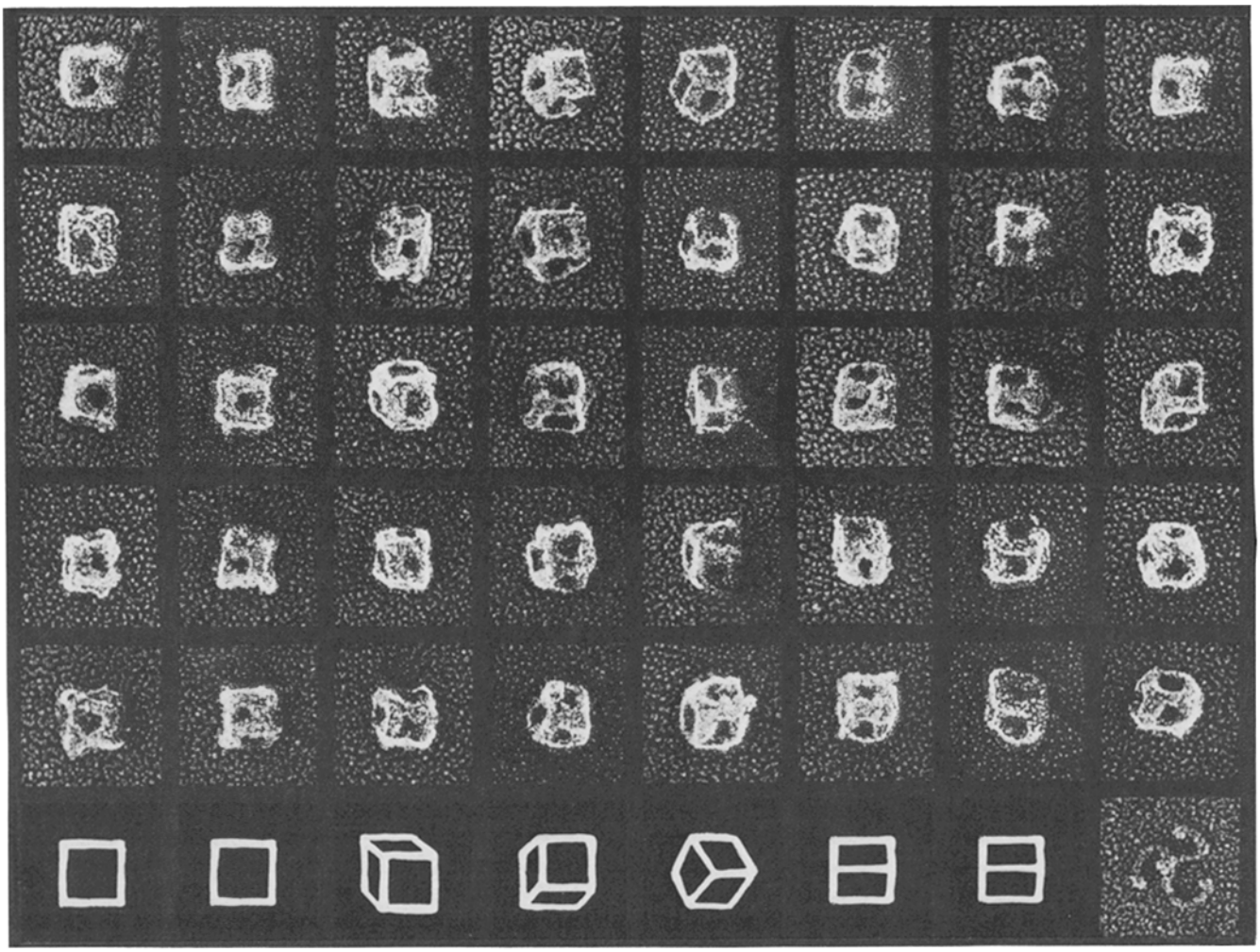

Figure 4. Gallery of different views of 42S clathrin polymers adsorbed to mica chips. Each column presents a slightly different view, epitomized by the drawings below; clearly, all represent different views of 33-nm cubes. The cubes are "clean" here because ammonium sulfate was washed away before quick-freezing, as in Fig. 3 (*lower panel*). (Curiously, this wash could not be done without provoking complete collapse of the cubes onto the mica, unless the mica was passed through 0.5% uranyl acetate for 30 s before washing. Such "fixation" of the cubes also seemed to be mandatory in the previous study on cubes [26].) The cubes shown here differ from those in reference 26 in that they are not collapsed by air drying and hence look smaller, measuring only 33 nm on a side as opposed to the value of 45 nm in reference 26. This brings them into line with the size of the tetrahedra shown above, and also with what would be expected from the actual length of a triskelion leg (10, 15). (Note the triskelion printed at the same magnification in the lower row.) Edge of each cube, 33 nm.

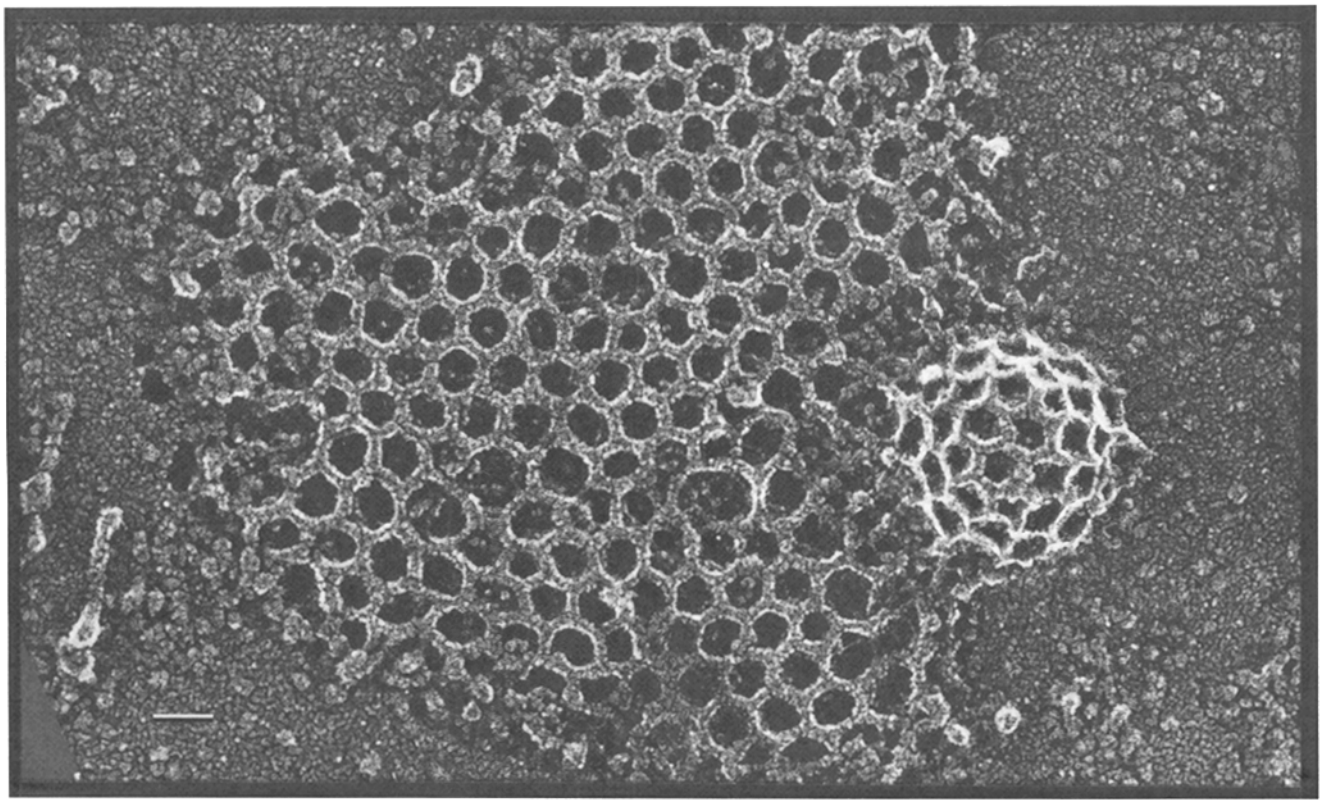

Figure 5. Deep-etch view of a typical clathrin lattice found on the inside of a tissue cultured cell, printed at the same magnification as the small clathrin polymers in Figs. 2 and 4 to permit direct comparison of their relative dimensions. (This happens to be from a human carcinoma cell chronically infected with measles virus, kindly provided by Dr. Monique du Bois-Dalcq, National Institute of Neurological, Communicative Disorders, and Stroke, National Institutes of Health.) Bar, 33 nm.

four triskelia lie in close proximity to each other but are no longer in intimate association (Fig. 11, row *b*). These provide compelling evidence that the 27S species are tetramers, not hexamers.

Because the images of tetrahedra collapsed on mica look so different from the earlier images of tetrahedra suspended in ice and partially exposed by etching, we collected a number of images that bridge the gap between the two (Figs. 12 and 13). These include examples of tetrahedra that have been only partially "melted" by contact with the polylysine mica, such that one vertex remains above the mica and displays three struts running down to the melted part (Fig. 13, row *a*). The elevated struts look thick and smooth, like those of suspended tetrahedra (Figs. 1 and 2), whereas the adsorbed portions look thinner and bipartite, like other collapsed species (Figs. 7 and 8).

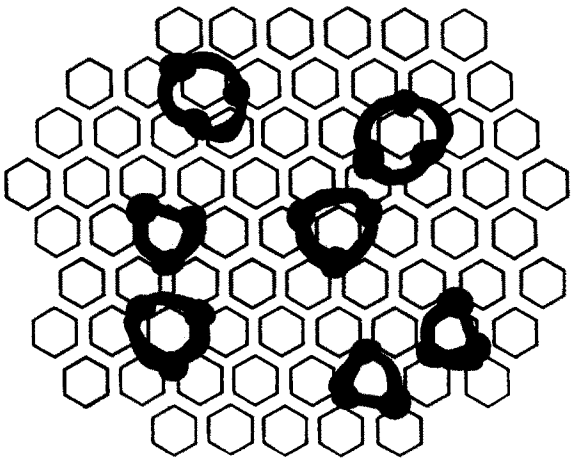

Figure 6. Camera lucida tracings of individual tetrahedral faces (from Fig. 2) superimposed on an identically scaled hexagonal lattice (as in Fig. 5), to illustrate that the tetrahedral vertices fall in register with non-adjacent vertices in the in situ lattice.

Other curious "intermediate" images were found in preparations of 27S clathrin that were placed on untreated mica while still in 2 mM MES buffer. As mentioned above, clathrin does not adsorb to mica under these conditions; but when etching is very deep, some tetrahedra are completely released from the ice and fall onto the mica during freeze-drying. Examples of such entities are shown in Fig. 13 (row *b*). These are obviously smaller than tetrahedra that remain supported by ice (Fig. 2), and look more irregular (like raisins compared to grapes), but they do display four distinct vertices with struts running among all of them, suggesting that they are tetrahedra that have collapsed internally.

Further Biochemical Characterization of 27S Clathrin

The earlier conclusion that 27S polymers are composed of six clathrin trimers was based on sedimentation equilibrium analysis (23). However, the electron microscopic data shown here indicated that the physical studies had to be repeated. In the course of these new experiments we learned that the

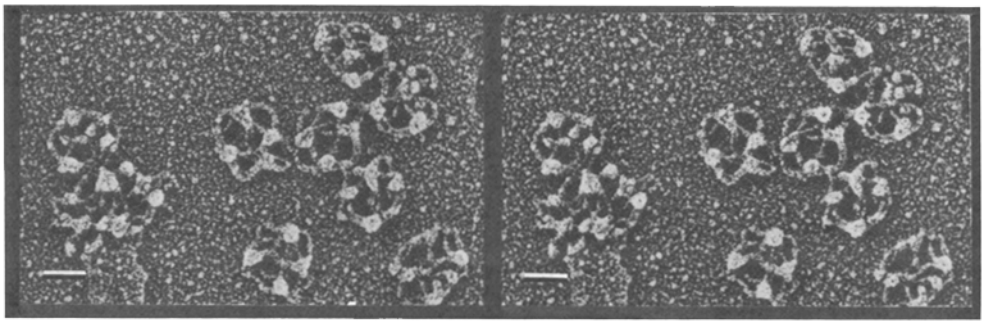

Figure 7. Stereo view of 27S clathrin tetrahedra fixed with glutaraldehyde and adsorbed to polylysine-pretreated mica before freeze-drying, to illustrate their collapse on mica. Bars, 33 nm.

27S polymer is stable in 2 mM MES, pH 5.9, for at least 3–4 wk at 4°C. However, samples stored for this length of time do not dissociate completely into 8S species when pH is raised to 8.0 or 2 M urea is added. Instead they form two distinctly sedimenting boundaries at 8–10S and 16–18S, with a concentration ratio of roughly 1:3 (analytical ultracentrifugation data, not shown). This implies that some contacts are becoming fixed or clathrin is slowly denaturing in the low

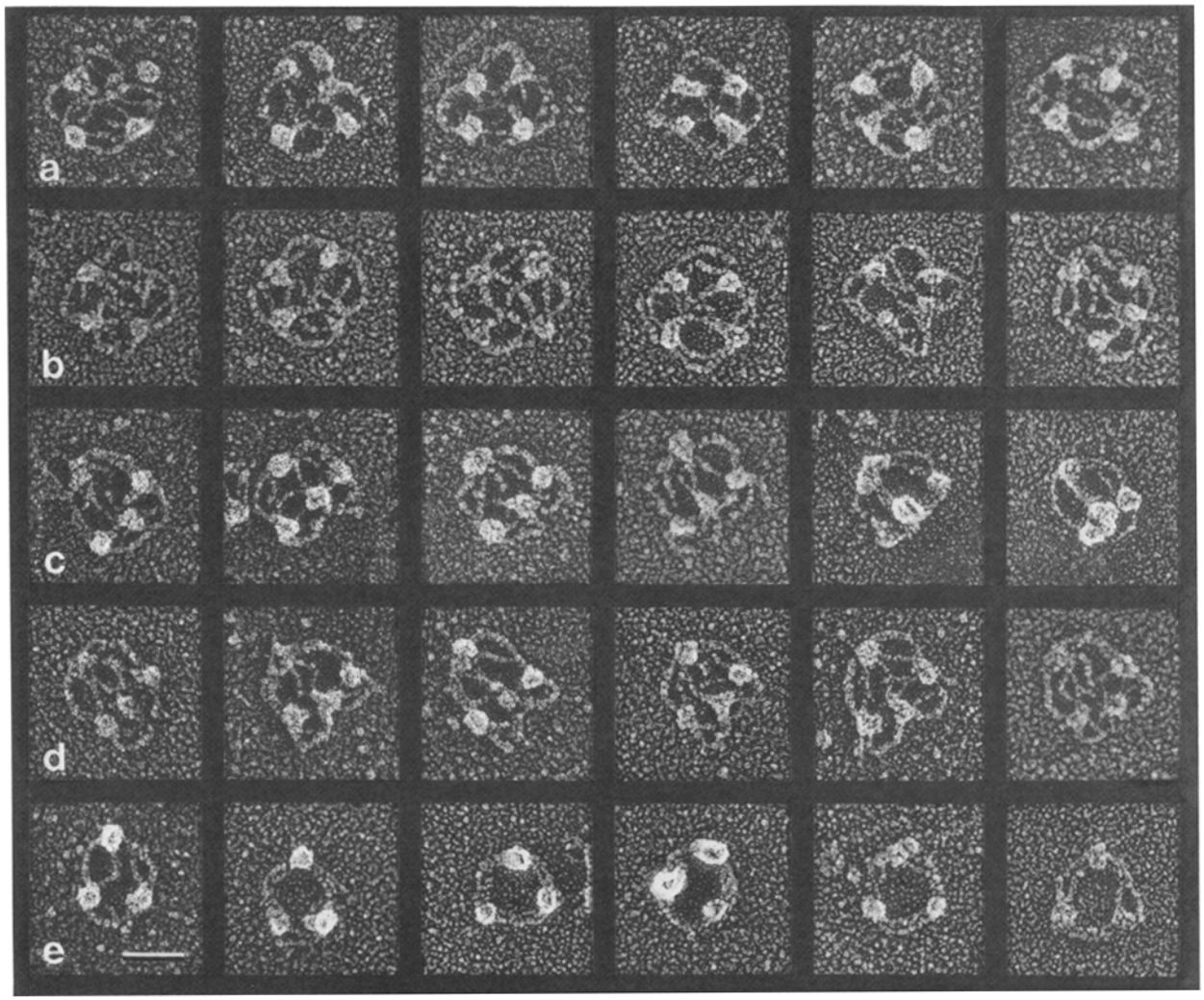

Figure 8. Gallery of individual 27S clathrin tetrahedra after fixation and adsorption to mica (as in Fig. 7). Row *a* depicts examples with four particularly distinct globules in a square array; row *b* depicts additional examples with near perfect radial symmetry and more clear-cut delineation of the 12 struts that interconnect the four globules; rows *c* and *d* illustrate others that have collapsed differently, such that three of their globules are aligned while the fourth is off to the side, thus yielding "medusae" images. The four globules are relatively prominent in row *c* while the 12 interconnecting struts are relatively prominent in row *d*. (Note that the patterns in *a* and *b* should result from tetrahedra striking the mica on one edge, while those in *c* and *d* should result from tetrahedra striking mica on one face; cf. Fig. 10.) Row *e* depicts our entire collection of some very rare variants in these preparations, in which only three globules and six struts are present. These may be formed out of proteolysed triskelia (cf. reference 10). Bar, 33 nm.

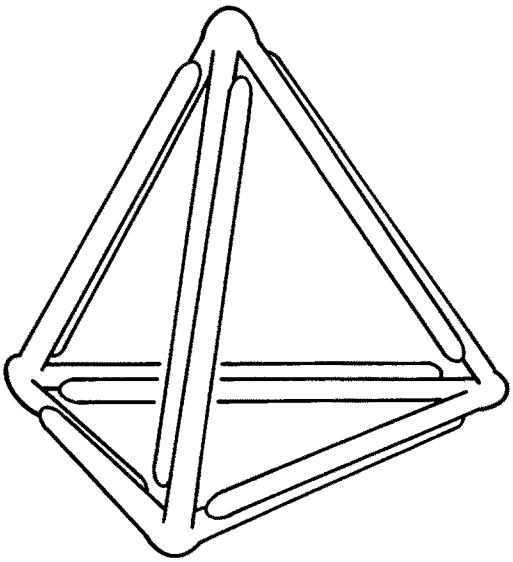

Figure 9. Diagram of the most likely way in which four clathrin triskelia could pucker their vertices and straighten their legs to form tetrahedra of the size found in 27S clathrin preparations. For simplicity, the terminal domains of the triskelial legs are omitted. Note that three of these terminal domains should come together underneath each vertex.

salt conditions. Whatever the process, its importance for the present study is that it apparently involves a concomitant aggregation of the 27S species. Upon review of our earlier centrifugation data, it became clear that our clathrin had undergone such changes and that much larger species were forming and spinning out during the ~1 wk centrifugation run. (We found that similar irreversible changes occur when normal 150S clathrin cages are placed in 2 mM MES at pH 5.9. After 2 d, they no longer dissociate completely into 8S species when pH is raised to 8.0 or 2 M urea is applied, but instead form two sedimenting boundaries, one corresponding to ~8S and the other ~40–70S, in about equal amounts.

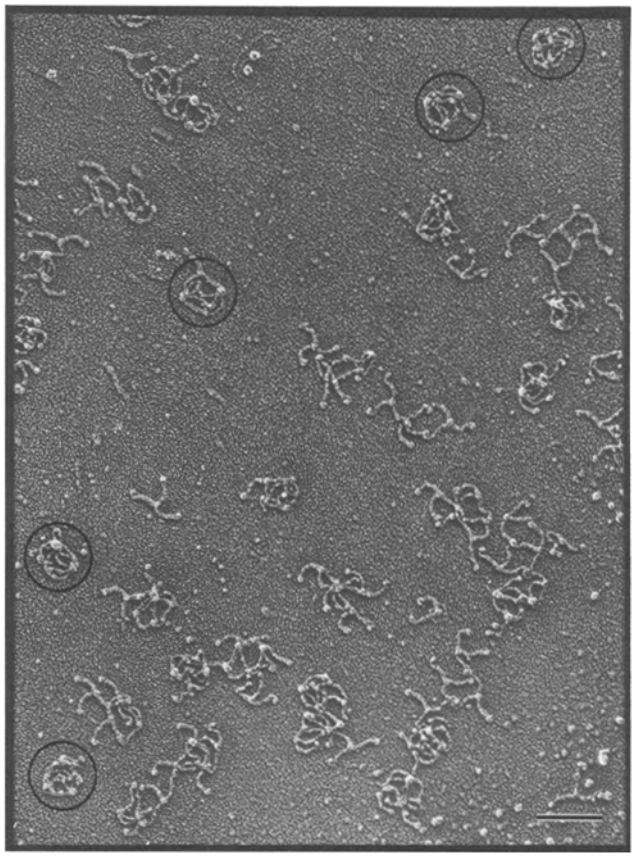

Figure 10. Survey view of 27S clathrin species falling apart on mica, to illustrate that they are each formed from four triskelions. Partial dissociation was provoked here by transferring a 27S preparation from 2 mM MES buffer to 70 mM KCl and 30 mM Hepes buffer pH 7.0 for 30 s before adsorption to mica. (This was done in an attempt to overcome mica's low affinity for clathrin in dilute solutions, but the dissociation shown here prompted the development of the alternative technique used for Figs. 7 and 8). Circles denote tetrahedra that are still relatively intact and look like those in Fig. 8. Bar, 0.1 μm.

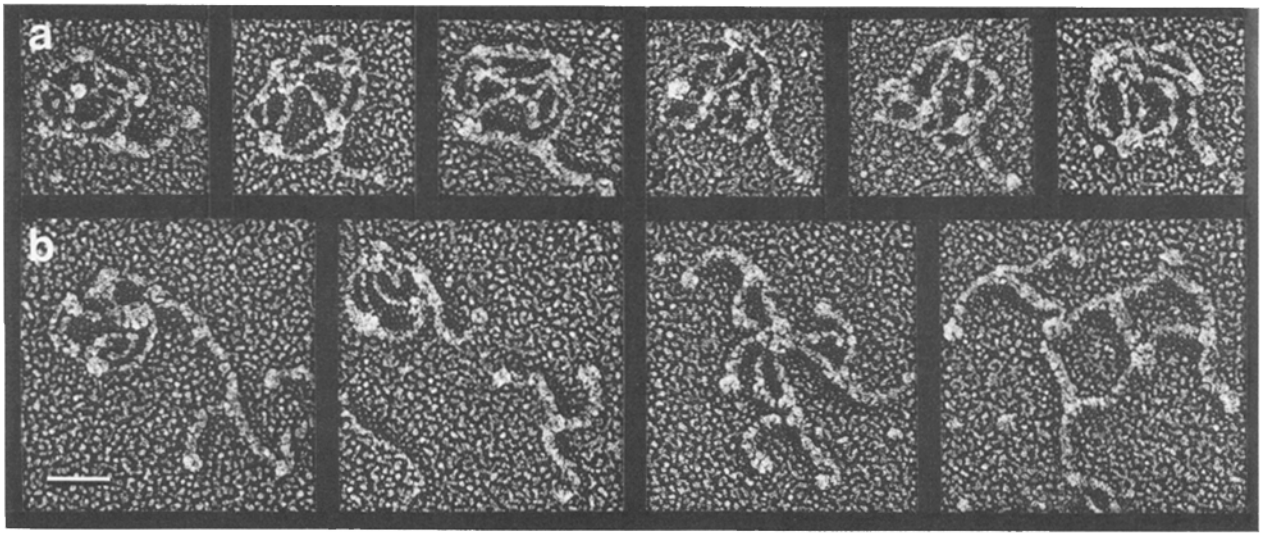

Figure 11. Gallery of high magnification views of 27S clathrin polymers releasing individual "legs" (*a*) or dissociating more completely into 4 distinguishable triskelia (*b*), selected from fields like Fig. 10. Bar, 33 nm.

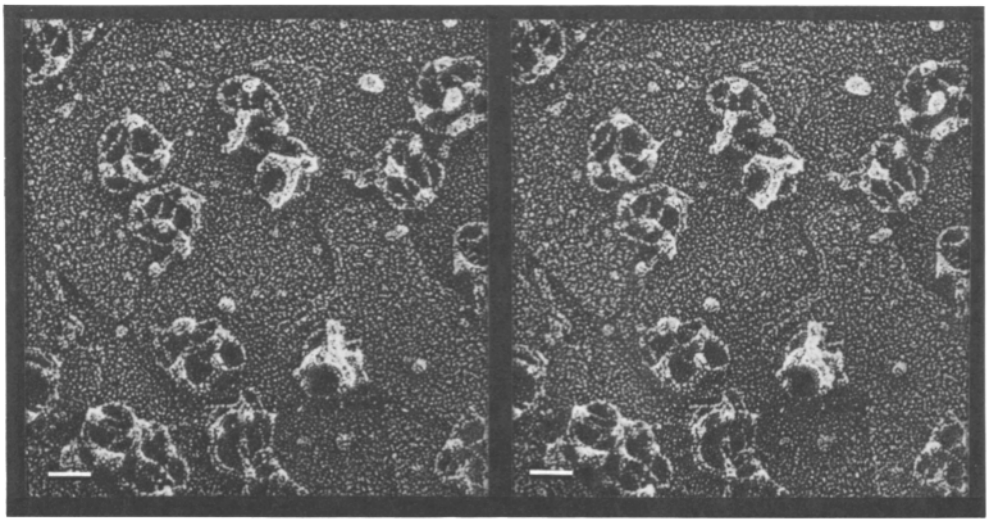

Figure 12. Stereo view of a field of prefixed 27S clathrin polymers that happened to adsorb to polylysine mica with less collapse than usual, thus leaving remnants of the normal tetrahedral strut arrangement on their portions that lie above the mica. Bar, 33 nm.

Neither dithiothreitol [DTT] nor mercaptoethanol prevents the above "aging" change in low ionic strength, indicating it does not result from disulfide bond formation.)

From the above observations it seems clear that some sort of irreversible change in clathrin occurs in 2 mM MES, pH 5.9. This does not occur at higher salt concentrations, but because 27S clathrin falls apart in higher salt, we looked for other solvent conditions that would protect it. Glycerol was a prime candidate because it is known to stabilize proteins through preferential interaction with them (6, 7, 16). When several concentrations of glycerol were tried, we found that 3 M glycerol permitted the continuing existence of both the 27S species and 150S baskets in 2 mM MES, pH 5.9, yet allowed them to dissociate completely into 8S clathrin even after 4 wk of storage at 4°C. We took advantage of this to improve our molecular weight determination, by carrying out centrifugation in 3 M glycerol.

Fig. 14 displays the sedimentation equilibrium pattern of 27S species in 2 mM MES (pH 5.9) with 3 M glycerol. The line is a best fit curve for a one-component analysis, giving a molecular weight of 2.26×10^6. The root mean square error for the fit was 0.006. Assuming a triskelion molecular weight of 630,000, this gives 3.6 triskelions per each 27S polymer. A second experiment under similar conditions, also with glycerol, gave a molecule weight corresponding to 3.8 triskelions. These data thus support the above electron microscopic evidence that the 27S species is a tetramer of triskelions. Since the curves indicate a single component, we made no attempt to analyze the data as a multicomponent system and thus to evaluate additional thermodynamic parameters, as we did in our earlier report (23).

Finally, we carried out light scattering experiments using Eq. 1 and 2 in the Materials and Methods to obtain an independent estimate of the molecular weight of the 27S species. To do this, a fresh solution of 27S clathrin in 2 mM MES, pH 5.9 at 0.1 mg/ml was titrated gradually to pH 8.0 with a concentrated solution of NaOH and light scatter values (Ir^2/I_0) were measured under both conditions. (We verified that these 27S species dissociated completely at pH 8.0 by analyzing the products in the analytical ultracentrifuge.) Blank values of the scatter for buffer alone were measured and subtracted at each pH. Three independent experiments gave scattering values of 76, 80, and 92 for the 27S polymer and 20, 22, and 26, for the 8S protomer, respectively. Since

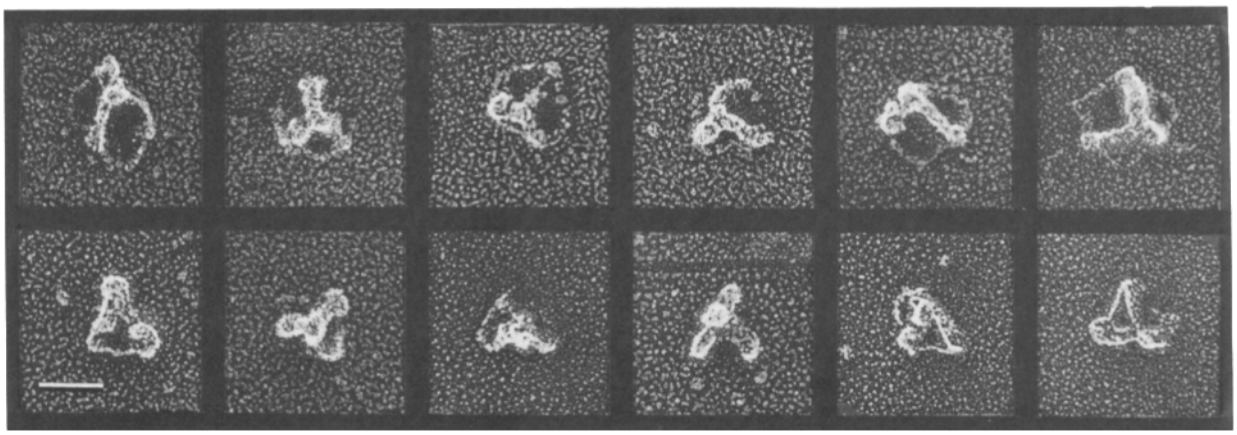

Figure 13. Gallery of 27S clathrin tetrahedra that did not fully collapse on mica. The top row includes selected examples from the preparation surveyed in Fig. 12. The bottom row is from a preparation mixed with mica in 2 mM MES, where adsorption did not occur, but in which some tetrahedra simply fell down onto the mica during the freeze-drying step. Bar, 33 nm.

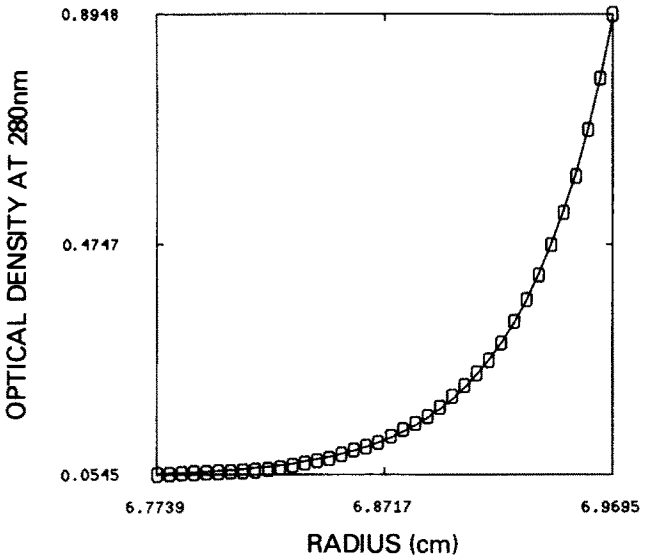

Figure 14. Equilibrium centrifugation pattern of 27S clathrin polymers in 2 mM MES pH 5.9, 3 M glycerol. The line represents the fit of the data for a single component (cf. reference 23).

the buffer conditions did not significantly change over this range of pHs, the H parameter could be assumed to be the same for both 27S and 8S forms (Eq. 2). Also, both forms are of comparable dimensions and much smaller than the wavelength of light used, and since both of them are fairly asymmetric, we assumed that $P(O)$ term did not vary significantly either. Finally, the experimental design ensured that the concentration term C for 27S and 8S forms stayed constant. Thus, from Eq. 1 we see that the relative ratio of their scattering values should indicate directly the ratio of their molecular weights. The above experimental values gave a ratio of 3.65 $\pm$ 0.20, again indicating that the 27S polymer is a tetramer of clathrin.

Discussion

Interpreting Images of Polymers in Suspension

The most likely interpretation of our images of 27S clathrin is that it forms a tetrahedron. Freeze-etching of 27S species in suspension has revealed various facets of what are clearly small, closed structures partially embedded in ice. Protruding from the ice are various views of faces that are invariably triangular and vertices that are invariably formed by the convergence of three struts. Tetrahedra are the only likely structures to generate such images (cf. Fig. 9).

Interpreting Images of 27S Clathrin on Mica

Unfortunately, 27S clathrin adsorbed to mica did not yield such definitive images. Unfixed tetrahedra fell apart completely on mica and glutaraldehyde-fixed ones collapsed internally during adsorption. Thereafter they looked somewhat like flattened projections of tetrahedra, but displayed certain differences that deserve mention. First, the flattened specimens invariably displayed four distinct globules that were not visible anywhere on tetrahedra in suspension. We imagine that these represent structures that were originally present inside the tetrahedron, hence invisible on metal replicas of their outsides. (Due to "self-shadowing" problems, evaporatively deposited metal rarely delineates anything down inside the openings of clathrin lattices, whether in situ or in vitro [8, 10].) The most likely candidates for such internal structures are the scroll-shaped "terminal domains" of the clathrin legs, which point inward in normal clathrin cages (10, 29, 30). Since each clathrin leg measures 45–50 nm in toto (10), while the struts in the tetrahedra measure only ~33 nm, quite a bit of each leg could be directed inward in them, as well. Indeed, the distance from any vertex to the very center of a tetrahedron is 0.55× the edge length (or 18 nm in these species), so if the remaining portions of each leg did radiate inward from each of the four vertices, they could probably touch each other in the center. Moreover, each vertex should represent the convergence of three terminal domains. Together, these would certainly provide enough mass to generate the large globules seen in collapsed tetrahedra.

A second discrepancy between adsorbed and suspended 27S clathrin is that the component struts in the latter are relatively smooth and display no hint of their supposed bipartite composition (e.g., two antiparallel triskelion legs; cf. Fig. 9). We presume that this is a problem resulting from the limited resolution of platinum replication in general. Replicas also fail to display any hint of the complicated overlap of four triskelion legs that ought to be present in the normal clathrin lattice (8, 10), and also give no hint of clathrin light chain presence or location (15). Only when a polymer's component parts are torn apart during adsorption to mica and deposited at a slight distance from each other do they become resolvable in metal replicas. For instance, such separation here demonstrates that 27S tetrahedra are composed of four triskelions, by clearly revealing four sets of triskelion components (four globular vertices and 12, i. e., four sets of three, interdigitated legs).

The relative dimensions of tetrahedra versus their component parts indicate that their four triskelia are probably in the straight-legged and highly "puckered" conformation diagrammed in Fig. 9. This differs in several respects from the arrangement postulated for normal clathrin baskets (4, 14, 27). In the normal basket, adjacent vertices are ~15 nm apart (5, 8, 12, 22), less than half the length of one triskelion leg, while in tetrahedra they are 33 nm apart. Isolated triskelia display distinct "kinks" at ~16 nm along each leg, marking the point at which each leg passes the adjacent vertex in the in situ cage and goes on to a second side (4, 10, 14, 15, 27). In tetrahedra, on the other hand, these "kinks" seem to be straightened out, since the vertices are separated by nearly twice this distance. Moreover, in tetrahedra the struts separate into only two legs upon adsorption to mica, while four legs overlap in each strut of a normal clathrin basket. Hence the correspondence in size between tetrahedra facets and basket facets shown in Fig. 6 can be misleading, in that one contains only half as many clathrin "building blocks" as the other. Furthermore, the three legs of each triskelion in a hexagonal basketwork are thought to radiate out from each vertex in one plane (when the network is completely flat as in the central portion of Fig. 5) or at most in a gentle "pucker" of some 15° off the plane (in more curved baskets like the icosahedral shells around brain coated vesicles; cf. references 10 and 14). In contrast, the triskelions in tetrahedra must be sharply puckered, each leg some 75° off of a plane

through the tetrahedral vertex. It would seem that a relatively flat, bent-legged 8S triskelion becomes converted, by the unique form of self-association that develops in very low ionic strength, into a very differently shaped entity, e.g., one that is highly puckered and straight-legged. This is the same transformation that has been postulated to occur during formation of the cubic 42S polymer (26).

Thus the 27S and 42S polymers of clathrin represent a remarkably similar pattern of assembly, even though one involves four triskelia and the other eight, and one forms in unusually low ionic strength while the other forms in unusually high ionic strength.

In our previous description of 27S species (23), the incorrect notion that they represented hexamers led to speculation that they might be intermediates in the assembly of normal cages, i.e., individual hexagonal "facets" like those found in normal in situ clathrin lattices. This would have fit with the prevailing view that the normal lattice contains one triskelion at each of the six vertices that form its hexagons (4, 14, 27). The problem with this view, however, is that deep-etched 27S species turn out to look like closed structures, while earlier workers have illustrated that fragments of baskets ought to be open structures bristling with uncommitted clathrin legs that can go on to overlap extensively with others in a completed network (4). We thus feel now that the entities under scrutiny here are probably not intermediates in normal clathrin lattice assembly. Since they only form in very unnatural ionic conditions, they are probably not related to any normal storage form of clathrin in the cytoplasm either, but that remains to be determined.

We thank Robyn Roth and Melisse Reichman for preparing the replicas, Cary Colman for photography, and Jan Jones for typing.

This work was supported largely by grant GM-29647 to J. Heuser from the National Institutes of Health.

Received for publication 13 April 1987, and in revised form 9 July 1987.

References

1. Blank, G. S., and F. M. Brodsky. 1986. Site-specific disruption of clathrin assembly produces novel structures. *EMBO (Eur. Mol. Biol. Organ.) J.* 5(9):2087–2095.
2. Blitz, A. L., R. E. Fine, and P. A. Toselli. 1977. Evidence that coated vesicles isolated from brain are calcium-sequestering organelles resembling sarcoplasmic reticulum. *J. Cell Biol.* 75:135–147.
3. Camerini-Otero, R. D., and L. A. Day. 1978. The wavelength dependence of the turbidity of solutions of macromolecules. *Biopolymers.* 17:2241–2249.
4. Crowther, R. A., and B. M. F. Pearse. 1981. Assembly and packing of clathrin into coats. *J. Cell Biol.* 91:790–797.
5. Crowther, R. A., J. T. Finch, and B. M. F. Pearse. 1976. On the structure of coated vesicles. *J. Mol. Biol.* 103:785–798.
6. DiPaola, G., and B. Belleau. 1978. Polyol-protein interactions. thermodynamical evidence for a selective solvation of glycerol and hexitols by aqueous β-lactoglobulin. *Can. J Chem.* 56:848–850.
7. Gekko, K., and S. N. Timasheff. 1981. Thermodynamic and kinetic examination of protein stabilization by glycerol. *Biochemistry.* 20:4677–4686.
8. Heuser, J. E. 1980. Three-dimensional visualization of coated vesicle formation in fibroblasts. *J. Cell Biol.* 84:560–583.
9. Heuser, J. E. 1983. Procedure for freeze-drying molecules adsorbed to mica flakes. *J. Mol. Biol.* 169:155–195.
10. Heuser, J., and T. Kirchhausen. 1985. Deep-etch views of clathrin assemblies. *J. Ultrastruct. Res.* 92:1–27.
11. Heuser, J. E., J. H. Keen, K. Prasad, R. E. Lippold, and M. S. Lewis. 1986. A new tetrahedral clathrin assembly. *J. Cell Biol.* 103:(5, Pt. 2): 53a. (Abstr.)
12. Kaneseki, T., and K. Kadota. 1969.The "vesicle in a basket." *J. Cell Biol.* 42:202–220.
13. Keen, J. H., M. C. Willingham, and I. H. Pastan. 1971. Clathrin-coated vesicles: isolation, dissociation and factor-dependent reassociation of clathrin baskets. *Cell.* 16:303–312.
14. Kirchhausen, T., and Harrison, S. C. 1981. Protein organization in clathrin trimers. *Cell.* 23:755–761.
15. Kirchhausen, T., S. C. Harrison, and J. Heuser. 1986. Configuration of clathrin trimers: evidence from electron microscopy. *J. Ultrastruct. Mol. Struct. Res.* 94:199–208.
16. Lee, J. C., and S. N. Timasheff. 1977. In vitro reconstitution of calf brain microtubules: effects of solution variables. *Biochemistry.* 16:1754–1764.
17. Lisanti, M. P., W. Schook, N. Moskowitz, C. Ores, and S. Puszkin. 1981. Brain clathrin and clathrin-associated proteins. *Biochem. J.* 201:297–304.
18. Lisanti, M. P., L. S. Shapiro, N. Moskowitz, E. L. Hua, S. Puszkin, and W. Schook. 1982. Isolation and preliminary characterization of clathrin-associated proteins. *Eur. J. Biochem.* 125:463–470.
19. Nandi, P. K., H. T. Pretorius, R. E. Lippoldt, M. L. Johnson, and H. Edelhoch. 1980. Molecular properties of the reassembled coat protein of coated vesicles. *Biochemistry.* 19:5917–5921.
20. Nandi, P. K., K. Prasad, R. E. Lippoldt, A. Alfsen, and H. Edelhoch. 1982. Reversibility of coated vesicle dissociation. *Biochemistry.* 21: 6434–6440.
21. Nossal, R., G. H. Weiss, P. K. Nandi, R. E. Lippoldt, and H. Edelhoch. 1983. Size and mass distributions of clathrin-coated vesicles from bovine brain. *Arch. Biochem. Biophys.* 226:593–603.
22. Pearse, B. M. F. 1978. On the structural and functional components of coated vesicles. *J. Mol. Biol.* 126:803–812.
23. Prasad, K., R. E. Lippoldt, H. Edelhoch, and M. S. Lewis. 1986. An intermediate polymer in the assembly of clathrin baskets. *Biochemistry.* 25: 5214–5219.
24. Pretorius, H. T., P. K. Nandi, R. E. Lippoldt, M. L. Johnson, J. H. Keen, I. Pastan, and H. Edelhoch. 1981. Molecular characterization of human clathrin. *Biochemistry.* 20:2777–2782.
25. Schook, W., S. Puszkin, W. Bloom, C. Ores, and S. Kochwa. 1979. Mechanochemical properties of brain clathrin: interactions with actin and α-actinin and polymerization into basketlike structures or filaments. *Proc. Natl. Acad. Sci. USA.* 76:116–120.
26. Sorger, P. K., R. A. Crowther, J. T. Finch, and B. M. F. Pearse. 1986. Clathrin cubes: an extreme variant of the normal cage. *J. Cell Biol.* 103: 1213–1219.
27. Ungewickell, E., and D. Branton. 1981. Assembly units of clathrin coats. *Nature (Lond.).* 289:420–422.
28. van Jaarsveld, P. P., P. K. Nandi, R. E. Lippoldt, H. Saroff, and H. Edelhoch. 1981. Polymerization of clathrin protomers into basket structures. *Biochemistry.* 20:4129–4135.
29. Vigers, G. P. A., R. A. Crowther, and B. M. F. Pearse. 1986. Three-dimensional structure of clathrin cages in ice. *EMBO (Eur. Mol. Biol. Organ.) J.* 5(3):529–534.
30. Vigers, G. P. A., R. A. Crowther, and B. M. F. Pearse. 1986. Location of the 100 kd-50 kd accessory proteins in clathrin coats. *EMBO (Eur. Mol. Biol. Organ.) J.* 5(9):2079–2085.
31. Woodward, M. P., and T. F. Roth. 1978. Coated vesicles: characterization, selective dissociation, and reassembly. *Proc. Natl. Acad. Sci. USA.* 75:4394–4398.
32. Woodward, M. P., and T. F. Roth. 1979. Influence of buffer ions and divalent cations on coated vesicle disassembly and reassembly. *J. Supramol. Struct.* 11:237–250.